

# Cell-autonomous reduction of CYFIP2 changes dendrite length, dendritic protrusion morphology, and inhibitory synapse density in the hippocampal CA1 pyramidal neurons of 17-month-old mice

Yoonhee Kim<sup>a\*</sup>, Ruiying Ma<sup>a,b\*</sup>, Yinhua Zhang<sup>a</sup>, Hyae Rim Kang<sup>a,b</sup>, U Suk Kim<sup>a</sup> and Kihoon Han <sup>a,b</sup>

<sup>a</sup>Department of Neuroscience, Korea University College of Medicine, Seoul, Republic of Korea; <sup>b</sup>BK21 Graduate Program, Department of Biomedical Sciences, Korea University College of Medicine, Seoul, Republic of Korea

## ABSTRACT

The cytoplasmic FMR1-interacting protein 2 (CYFIP2) have diverse molecular functions in neurons, including the regulation of actin polymerization, mRNA translation, and mitochondrial morphology and function. Mutations in the *CYFIP2* gene are associated with early-onset epilepsy and neurodevelopmental disorders, while decreases in its protein levels are linked to Alzheimer's disease (AD). Notably, previous research has revealed AD-like phenotypes, such as dendritic spine loss, in the hippocampal CA1 pyramidal neurons of 12-month-old *Cyfp2* heterozygous mice but not of age-matched CA1 pyramidal neuron-specific *Cyfp2* conditional knock-out (cKO) mice. This study aims to investigate whether dendritic spine loss in *Cyfp2* cKO mice is merely delayed compared to *Cyfp2* heterozygous mice, and to explore further neuronal phenotypes regulated by CYFIP2 in aged mice. We characterized dendrite and dendritic protrusion morphologies, along with excitatory/inhibitory synapse densities in CA1 pyramidal neurons of 17-month-old *Cyfp2* cKO mice. Overall dendritic branching was normal, with a reduction in the length of basal, not apical, dendrites in CA1 pyramidal neurons of *Cyfp2* cKO mice. Furthermore, while dendritic protrusion density remained normal, alterations were observed in the length of mushroom spines and the head volume of stubby spines in basal, not apical, dendrites of *Cyfp2* cKO mice. Although excitatory synapse density remained unchanged, inhibitory synapse density increased in apical, not basal, dendrites of *Cyfp2* cKO mice. Consequently, a cell-autonomous reduction of CYFIP2 appears insufficient to induce dendritic spine loss in CA1 pyramidal neurons of aged mice. However, CYFIP2 is required to maintain normal dendritic length, dendritic protrusion morphology, and inhibitory synapse density.

## ARTICLE HISTORY

Received 17 April 2024  
Revised 18 May 2024  
Accepted 22 May 2024

## KEYWORDS

CYFIP2; CA1 pyramidal neuron; dendrite; dendritic spine; synapse

## Introduction


The cytoplasmic FMR1-interacting protein family, comprising CYFIP1 and CYFIP2, are evolutionarily conserved multifunctional proteins, and their dysfunction is causally associated with various brain disorders, including autism spectrum disorders, intellectual disability, schizophrenia, and early-onset epilepsy (Schenck et al. 2001; Abekhoukh and Bardoni 2014; Zhang, Lee, et al. 2019; Kang et al. 2023). At the molecular level, CYFIP1/2 is a core component of the heteropentameric Wiskott – Aldrich syndrome protein family verprolin-homologous protein (WAVE) regulatory complex (WRC) that regulates actin polymerization and branching in various cell types (Chen ZC et al. 2010; Lee Y et al. 2017; Rottner et al. 2021). Additionally, CYFIP1/2 have been reported to

have other molecular functions, such as regulating mRNA translation and transport (Napoli et al. 2008; De Rubeis et al. 2013; Cioni et al. 2018; Lee Y et al. 2020), and influencing mitochondrial morphology and function (Kanellopoulos et al. 2020; Kim GH et al. 2020). These functions are primarily mediated by other protein interactors of CYFIP1/2 and are possibly independent of the WRC.

Despite our knowledge of these molecular functions, further investigation is required to understand the specific neuronal phenotypes affected by CYFIP1/2. Notably, CYFIP1 and CYFIP2 proteins are found in both excitatory and inhibitory synaptic compartments of neurons (Pathania et al. 2014; Davenport et al. 2019). Moreover, given the crucial role of the actin cytoskeleton

**CONTACT** Kihoon Han  neurohan@korea.ac.kr

\*Yoonhee Kim and Ruiying Ma contributed equally to this work.

 Supplemental data for this article can be accessed online at <https://doi.org/10.1080/19768354.2024.2360740>.

© 2024 The Author(s). Published by Informa UK Limited, trading as Taylor & Francis Group

This is an Open Access article distributed under the terms of the Creative Commons Attribution-NonCommercial License (<http://creativecommons.org/licenses/by-nc/4.0/>), which permits unrestricted non-commercial use, distribution, and reproduction in any medium, provided the original work is properly cited. The terms on which this article has been published allow the posting of the Accepted Manuscript in a repository by the author(s) or with their consent.

in regulating neuronal dendritic development (Konietzny et al. 2017), it is conceivable that CYFIP1/2 may also play a part in this process. Indeed, some studies have shown morphological and functional changes in excitatory and inhibitory synapses, as well as alterations in dendritic structures, when the expression of CYFIP1 is either decreased or increased in mouse brains or cultured neurons (Pathania et al. 2014; Oguro-Ando et al. 2015; Davenport et al. 2019). However, when it comes to CYFIP2, such phenotypes have been explored to a lesser extent, although there are reports suggesting alterations in the morphology of dendritic spines (the dendritic protrusions where excitatory synapses are formed) in *Cyfp2* mutant mice (Han K et al. 2015; Lee SH et al. 2020; Zhang et al. 2020; Ma et al. 2023).

Beyond the identified genetic association of *CYFIP2* with neurodevelopmental disorders (Begemann et al. 2021), recent studies have revealed a mechanistical connection between reduced CYFIP2 levels and Alzheimer's disease (AD) (Tiwari et al. 2016; Ghosh et al. 2020). Notably, CYFIP2 proteins were found to be down-regulated in the postmortem forebrain of AD patients and in the hippocampus and cortex of AD model mice (Tiwari et al. 2016). Additionally, aged (12-month-old) *Cyfp2* heterozygous mice exhibited several AD-like phenotypes in the hippocampus, including increased levels of Tau phosphorylation, gliosis, and loss of dendritic spines in CA1 pyramidal neurons (Ghosh et al. 2020). Mechanistically, the diminished expression of CYFIP2 leads to aberrant mRNA translation of various AD-related proteins at the synaptic compartment, resulting in the overproduction of A $\beta$  and hyperphosphorylation of Tau in *Cyfp2* heterozygous mice. Intriguingly, a recent study showed that 12-month-old *Cyfp2* conditional knock-out (cKO, *Cyfp2*<sup>floxex/floxex</sup>; *CaMKII $\alpha$ -Cre* T29-1 (Tsien et al. 1996)) mice, which specifically reduce CYFIP2 protein levels in CA1, but not CA3, pyramidal neurons of the hippocampus, do not exhibit AD-like phenotypes (Ma et al. 2023). These cKO mice displayed normal levels of phospho-Tau, gliosis, and dendritic spines (with a subtle reduction in thin spines of basal dendrites) in the hippocampus when compared to age-matched wild-type mice. This implies that a cell-autonomous reduction of CYFIP2 is not sufficient to induce AD-like phenotypes.

Nevertheless, there is the possibility that AD-like abnormalities, such as dendritic spine loss, could be merely delayed in *Cyfp2* cKO mice compared to *Cyfp2* heterozygous mice (Ma et al. 2023). Consequently, these defects may become apparent in cKO mice beyond the age of 12 months. Moreover, an exploration of excitatory and inhibitory synapses, along with

dendritic structures, in aged *Cyfp2* cKO mice could provide further insights into the neuronal phenotypes affected by CYFIP2. To address these issues, our study explores CA1 pyramidal neurons in 17-month-old *Cyfp2* cKO mice through a combination of immunohistochemistry and 3D morphological analysis.

## Materials and methods

### Mice

The *Cyfp2* cKO (*Cyfp2*<sup>floxex/floxex</sup>; *CaMKII $\alpha$ -Cre* T29-1) mice used in this study were previously described (Lee SH et al. 2020; Zhang et al. 2020; Ma et al. 2023). *Thy1-YFP* [B6.Cg-Tg(Thy1-YFP)HJrs/J] mice were obtained from the Jackson Laboratory and bred with *Cyfp2* cKO mice as previously described (Zhang et al. 2020). The mice were bred and maintained in a C57BL/6J background (Japan SLC, Inc., Shizuoka, Japan) according to the Korea University College of Medicine Research Requirements. All procedures were approved by the Committee on Animal Research of the Korea University College of Medicine (KOREA-2018-0174). The mice were fed ad libitum and housed under a 12 h light–dark cycle. All experiments were performed using four pairs of aged (17-month-old) male *Cyfp2* cKO;*Thy1-YFP* mice and their littermate controls (*Cyfp2*<sup>floxex/floxex</sup> without Cre expression;*Thy1-YFP*).

### Fluorescence immunohistochemistry

Fluorescence immunohistochemistry was performed as previously described (Choi et al. 2015; Lee B et al. 2017; Zhang, Kang, et al. 2019; Kim HJ et al. 2022; Ma et al. 2022). Mice were anesthetized with isoflurane and transcardially perfused with heparinized (20 units/mL) phosphate-buffered saline (PBS), followed by 4% paraformaldehyde (PFA) in PBS. The brains were extracted and post-fixed overnight in 4% PFA. Following post-fixation, brain tissue was washed with PBS and cryoprotected with 30% sucrose in PBS for 48 h. The brain tissues were frozen in an O.C.T compound (SAKURA Tissue-Tek, 4583) and sectioned (100  $\mu$ m) using a cryostat microtome (Leica, CM3050S). The sections were collected and stored in 50% glycerol in 2 $\times$  PBS at  $-20^{\circ}\text{C}$  until further processed. The primary antibodies used for immunohistochemistry were CYFIP2 (Abcam, #AB95969), GFP (Abcam, #AB13970), Gephyrin (Synaptic Systems, #147011), Homer1 (Synaptic Systems, #160002), NeuN (Abcam, #AB177487; Millipore, #MAB377), Parvalbumin (Swant, #PV235), Somatostatin (Millipore, #MAB354), vGAT (Synaptic Systems, #131004), and vGlut1 (Millipore, #AB5905). The

secondary antibodies used were Alexa Fluor-conjugated (Jackson ImmunoResearch Labs). The samples were washed with 0.1% Triton X-100 in PBS and blocked with PBS containing 3% bovine serum albumin (BSA) and 0.5% Triton X-100. Finally, the sections were mounted on slide glasses with mounting media (Biomedica, M02).

### Dendritic morphology analysis

Images of entire dendritic branches of CA1 pyramidal neurons were acquired by confocal microscopy (Zeiss, LSM900,  $\times 20$  objective (0.8 numerical aperture),  $\times 0.6$  digital zoom, 16-bit image depth, and Z-stack function with 1  $\mu\text{m}$  intervals, total 28–30  $\mu\text{m}$  thickness) and were analyzed using Imaris 10.0.1 (Bitplane, UK). The Imaris Filament Tracer Module was utilized for detecting and analyzing dendritic structures. Two to three neurons were imaged from each mouse.

### Dendritic protrusion and excitatory/inhibitory synapse analysis

Images of dendritic segments with a length longer than 30  $\mu\text{m}$  of CA1 pyramidal neurons were acquired by confocal microscopy (Zeiss, LSM900,  $\times 63$  objective (1.2 numerical aperture),  $\times 3$  digital zoom, 16-bit image depth, Z-stack function with 0.2  $\mu\text{m}$  intervals, total 3–4.5  $\mu\text{m}$  thickness) and were analyzed using Imaris 10.0.1 (Bitplane, UK). The Imaris Filament Tracer Module was employed to detect, quantify, and classify dendritic protrusions, while the Spot Detection Function was utilized for detecting and analyzing excitatory and inhibitory synaptic puncta. Dendritic protrusion types were categorized as shown in Table 1. Two to three neurons were imaged from each mouse.

### Statistical analysis

All quantifications were performed by researchers who were blinded to the genotype and did not participate in immunostaining or image acquisition processes. *P* values were calculated using either a two-way ANOVA with Šídák's multiple comparisons test (recommended

by the software for sholl analysis due to its higher power compared to the Bonferroni test) or a two-tailed Student's *t*-test performed with GraphPad Prism 9 software. All data are presented as mean  $\pm$  standard error of the mean (SEM). \**P* < 0.05; \*\*\**P* < 0.001.

## Results

### Reduced length of the basal, but not apical, dendrites of CA1 pyramidal neurons in 17-month-old *Cyfp2* cKO mice

Before investigating detailed neuronal morphologies, we first validated the downregulation of CYFIP2 levels in the hippocampal CA1 region of 17-month-old *Cyfp2* cKO mice compared to control mice through immunohistochemistry (Figure 1A). Similar to findings from 12-month-old *Cyfp2* cKO mice (Ma et al. 2023), CYFIP2 levels decreased by approximately 50% in cKO mice compared to control mice. The remaining CYFIP2 signals detected in cKO mice might arise from the expression of CYFIP2 in inhibitory neurons (Lee SH et al. 2020) and/or technical background noise in the immunostaining process. Indeed, we observed CYFIP2 signals in excitatory pyramidal neurons as well as Parvalbumin – or Somatostatin-positive inhibitory neurons of the hippocampal CA1 region of 17-month-old control mice (Supplementary Figure 1). As previously demonstrated (Zhang et al. 2020; Ma et al. 2023), yellow fluorescent protein (YFP) expression in Thy-1 mice facilitated the visualization of CA1 pyramidal neuron morphology in both control and cKO mice (Figure 1A).

The Filament Tracer Module of Imaris software was employed to analyze dendritic morphology, automatically detecting and quantifying dendrites from Z-stack images of CA1 pyramidal neurons. Sholl analysis for total (combining basal and apical), basal, or apical dendrites revealed a comparable number of intersections in the CA1 pyramidal neurons of *Cyfp2* cKO mice compared to control mice (Figure 1B). Similarly, there was no significant difference in the number of dendritic branch points between cKO mice and control mice (Figure 1C). However, the length notably decreased for basal dendrites in cKO mice compared to control mice, while no significant changes were observed in total and apical dendrites (Figure 1D).

### Morphological changes of dendritic protrusions in the basal, but not apical, dendrites of CA1 pyramidal neurons in 17-month-old *Cyfp2* cKO mice

Next, we investigated dendritic protrusions in the CA1 pyramidal neurons of 17-month-old *Cyfp2* cKO mice.

**Table 1.** Classification of dendritic protrusion morphology using Imaris 10.1.0.

Type	Parameter
Mushroom spines	mean width (head) > mean width (neck)
Stubby spines	length (spine) < 1 $\mu\text{m}$
Long-thin spines	mean width (neck) $\times 2$ < length (spine) and mean width(neck) $\leq$ max width (head)
Filopodia	mean width (head) $\leq$ mean width (neck)

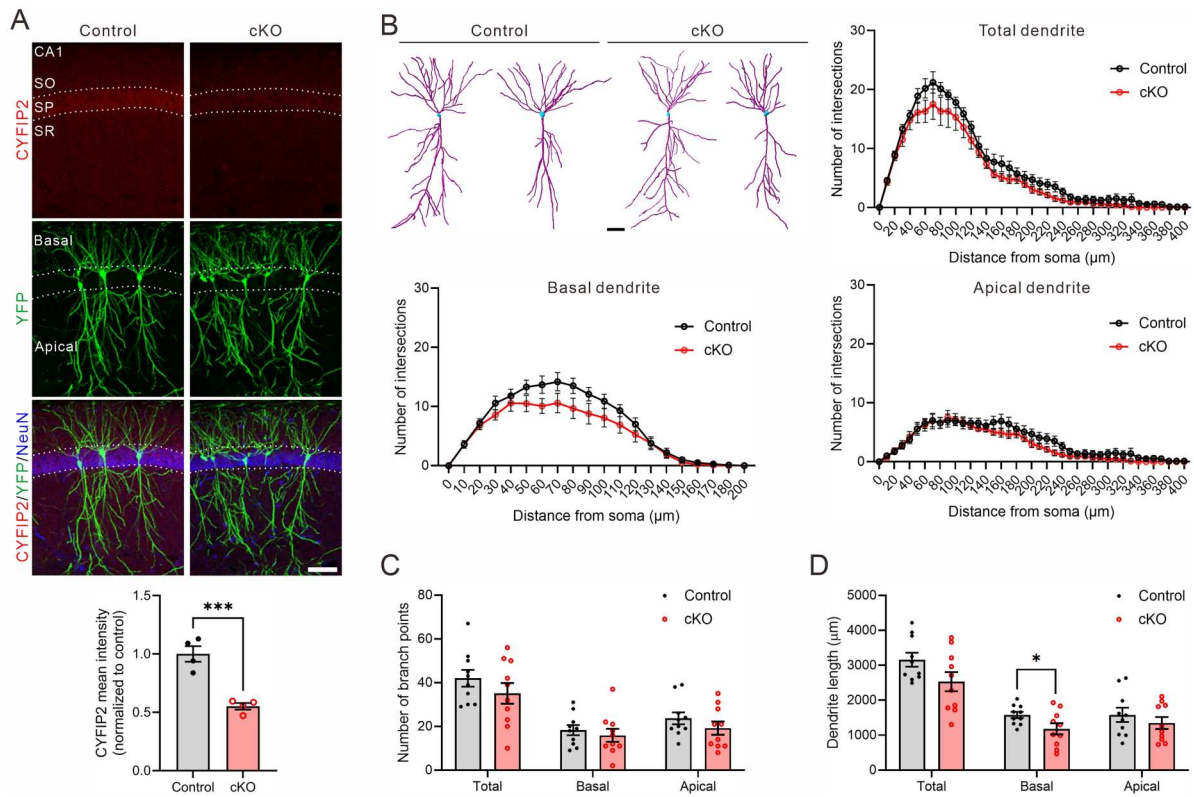


**Figure 1.** Dendritic morphology of CA1 pyramidal neurons in 17-month-old *Cyfip2* cKO mice. (A) Representative confocal images of CYFIP2, YFP, and NeuN immunofluorescent staining in the hippocampal CA1 region of 17-month-old control (*Cyfip2*<sup>flxed/flxed</sup>; *Thy1-YFP*) and *Cyfip2* cKO (*Cyfip2*<sup>flxed/flxed</sup>; *CaMKII $\alpha$ -Cre*; *Thy1-YFP*) mice. Quantification of CYFIP2 mean intensity in the stratum pyramidale (SP) layer. CA, cornu ammonis; DG, dentate gyrus; SO, stratum oriens; SR, stratum radiatum. Scale bar, 100  $\mu\text{m}$ . (B) Representative dendritic morphologies (traced by Imaris) of CA1 pyramidal neurons in 17-month-old control and *Cyfip2* cKO mice. Scale bar, 40  $\mu\text{m}$ . Quantification of Sholl analysis (for total, basal, and apical dendrites). (C) Quantification of dendritic branch points. (D) Quantification of dendritic length. N = 10 neurons per genotype.

We conducted separate analyses for dendritic protrusions in both basal and apical dendrites, building upon previous findings from 12-month-old *Cyfip2* cKO mice, which revealed reductions in total protrusion and thin spine densities in basal, but not apical, dendrites (Ma et al. 2023). From the confocal Z-stack images of dendritic segments, protrusions were automatically detected, classified into mushroom, stubby, and long thin spines, as well as filopodia (Table 1), and their size and volume were analyzed by Imaris software (Figure 2A).

In terms of dendritic protrusion density, no significant difference was observed in either the total (average of all protrusions) or any subclass of protrusions between control and cKO mice in both basal and apical dendrites (Figure 2B). However, in basal dendrites, both total and mushroom spines exhibited increased length in cKO mice compared to the control mice (Figure 2C). Conversely, there was no difference in length for any subclass of protrusions in apical dendrites between control and cKO mice. Similarly, only stubby spines in basal, but not apical, dendrites of cKO mice showed reduced head volume compared to the control mice (Figure 2D).

Finally, the total volume, including head and neck, for any subclass of protrusions in both basal and apical dendrites was comparable between control and cKO neurons (Figure 2E).

### **Inhibitory, but not excitatory, synaptic changes in the apical dendrites of CA1 pyramidal neurons in 17-month-old *Cyfip2* cKO mice**

In addition to morphological analyses of CA1 pyramidal neurons, we investigate the quantity of excitatory and inhibitory synapses in both basal and apical dendrites of 17-month-old *Cyfip2* cKO mice. Excitatory presynaptic compartments were identified using antibodies against vesicular glutamate transporter 1 (vGlut1), while postsynaptic compartments were labeled with Homer1 antibodies. Conversely, inhibitory presynaptic compartments were marked by antibodies targeting vesicular gamma-aminobutyric acid (GABA) transporter (vGAT), and postsynaptic compartments were identified using Gephyrin antibodies. Following a methodology similar to dendritic spine analysis, confocal Z-stack



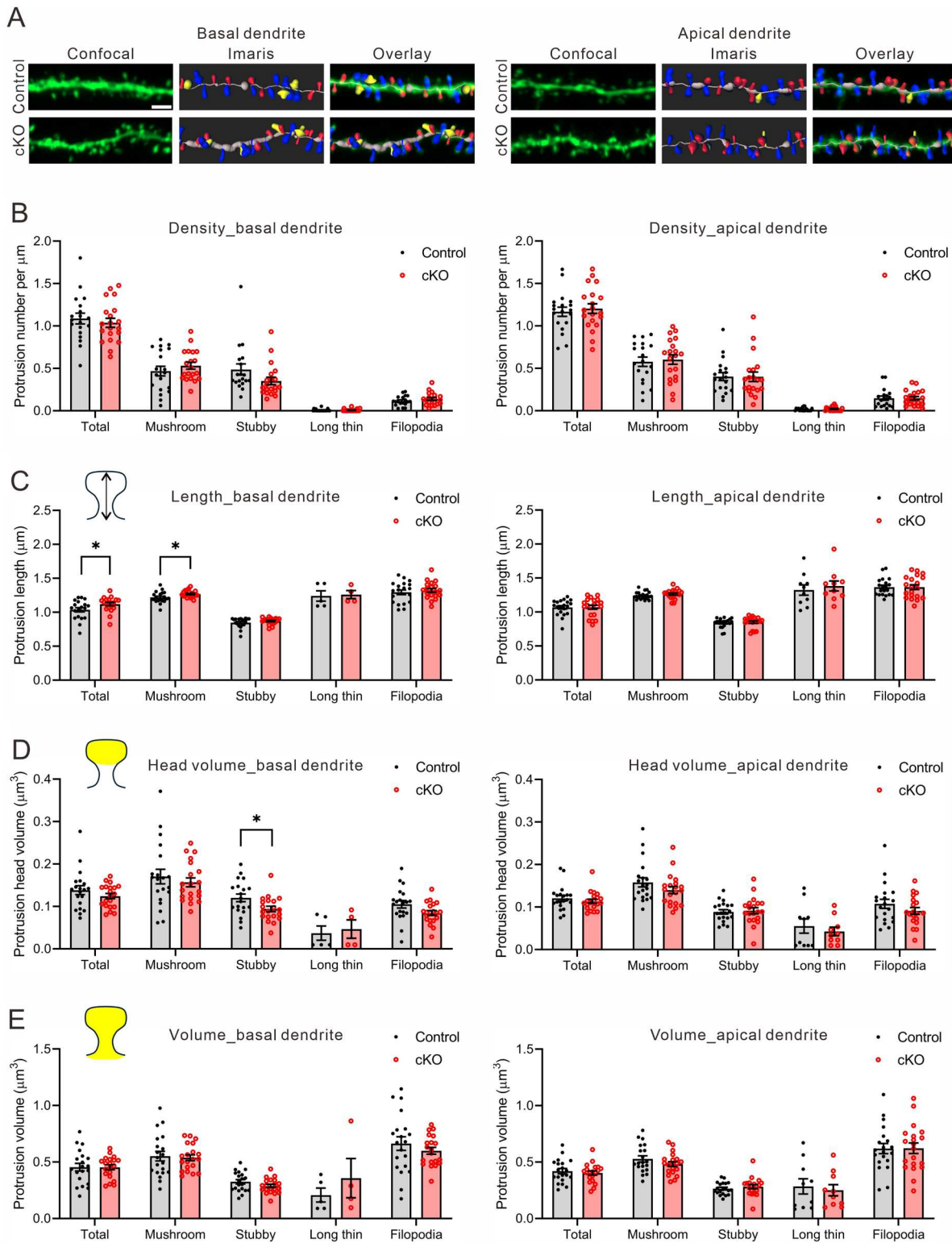


**Figure 2.** Dendritic protrusion density and morphology in CA1 pyramidal neurons of 17-month-old *Cyfp2* cKO mice. (A) Representative confocal images of dendritic protrusions and their Imaris classifications (blue for mushroom spine, red for stubby spine, yellow for filopodia) in both basal and apical dendrites of CA1 pyramidal neurons of 17-month-old control and *Cyfp2* cKO mice. Scale bar, 2  $\mu\text{m}$ . (B) Quantification of dendritic protrusion density in the basal (left panel) and apical (right panel) dendrites. (C) Quantification of dendritic protrusion length in the basal and apical dendrites. (D) Quantification of dendritic protrusion head volume in the basal and apical dendrites. (E) Quantification of dendritic protrusion total volume in the basal and apical dendrites.  $N = 20$  neurons per genotype.

images of dendritic segments were processed using Imaris software to automatically detect and quantify presynaptic and postsynaptic puncta associated with YFP-positive dendritic segments (Figure 3A and B). Specifically, only postsynaptic puncta contained within the volume of YFP-positive dendritic segments were considered. Presynaptic puncta within a 0.7  $\mu\text{m}$  distance from the surface of YFP-positive dendritic segments were included. Excitatory or inhibitory synapses were defined as instances where corresponding presynaptic and postsynaptic puncta were colocalized.

For excitatory synapses, neither the densities of vGlut1 puncta, Homer1 puncta, nor their colocalization (indicating excitatory synapses) showed significant differences between control and cKO mice, observed in both basal and apical dendrites (Figure 3A). Conversely, concerning inhibitory synapses, there were no abnormalities detected in the densities of vGAT puncta, Gephyrin puncta, nor their colocalization (indicating inhibitory synapses) in the basal dendrites of cKO mice (Figure 3B). However, notably, the density of inhibitory synapses significantly increased in the apical dendrites of cKO mice compared to control mice. While both vGAT and Gephyrin puncta densities displayed trends of increase in the apical dendrites of cKO mice compared to control mice, these differences did not reach statistical significance.

## Discussion

In this study, our aim was to investigate neuronal phenotypes, primarily focusing on morphological features, of hippocampal CA1 pyramidal neurons in 17-month-old *Cyfp2* cKO mice. We first observed a normal dendritic complexity, with a specific decrease in the length of basal dendrites in cKO mice. Reduction in dendritic complexity and length is a hallmark phenotype observed in the hippocampal CA1 pyramidal neurons of AD brains (Kulkarni and Firestein 2012; Mehder et al. 2020). Therefore, although confined to basal dendrites, the reduced dendritic length in pyramidal neurons of cKO mice may further suggest the link between CYFIP2 and AD pathologies. Furthermore, these findings align somewhat with a previous study showing that the overexpression of CYFIP2 in cultured hippocampal neurons leads to increased dendritic complexity and length (Pathania et al. 2014). The milder phenotype observed with CYFIP2 reduction in cKO mice compared to CYFIP2 overexpression in cultured neurons could potentially be attributed to compensation by CYFIP1, which likely contributes to maintaining normal dendritic structure in cKO mice. Indeed, previous research has indicated the involvement of CYFIP1 in regulating dendritic morphology

(Pathania et al. 2014; Davenport et al. 2019). However, it is also possible that CYFIP1 and CYFIP2 have distinct roles in regulating dendritic morphology, particularly during early development. For instance, it has been demonstrated that during the axonal development of retinal ganglion cells, CYFIP1 mediates axon growth while CYFIP2 regulates axon sorting (Cioni et al. 2018).

Our analysis of dendritic protrusions revealed normal densities of total and any subclass of protrusions in both basal and apical dendrites of CA1 pyramidal neurons of 17-month-old *Cyfp2* cKO mice. Consistently, densities of excitatory synapses (vGlut1-Homer1 colocalization), predominantly forming on dendritic spines, appeared normal in both basal and apical dendrites of cKO mice. These results suggest that dendritic spine loss is not simply delayed in *Cyfp2* cKO mice compared to 12-month-old *Cyfp2* heterozygous mice (Tiwari et al. 2016; Ghosh et al. 2020). Instead, they confirm that the cell-autonomous reduction of CYFIP2 is insufficient to induce dendritic spine loss in the hippocampal CA1 pyramidal neurons of *Cyfp2* cKO mice (Ma et al. 2023). Therefore, as hypothesized in the previous study (Ma et al. 2023), the loss of CYFIP2 in both pre- (e.g. CA3 pyramidal neurons or local inhibitory neurons) and post- (i.e. CA1 pyramidal neurons) synaptic neurons, occurring in *Cyfp2* heterozygous mice, might be necessary to fully induce dendritic spine loss in CA1 pyramidal neurons of aged mice. The role of CYFIP2 in presynaptic function has been less extensively characterized compared to its role in the postsynapse. Nevertheless, a previous study demonstrated an enhancement of presynaptic short-term plasticity induced by high-frequency stimuli in the medial prefrontal cortex (mPFC) layer 5 pyramidal neurons of adult (6–10-week-old) *Cyfp2* heterozygous mice, possibly associated with a reduced number of mitochondria in presynaptic boutons (Kim GH et al. 2020). Further investigation is required to understand whether and how CYFIP2 regulates presynaptic function and morphology in CA1 pyramidal neurons, as well as its potential interaction with the postsynaptic compartment to maintain a normal number of dendritic spines (Han KA and Ko 2023).

In line with the previous analysis of 12-month-old *Cyfp2* cKO mice (Ma et al. 2023), morphological changes (length and head volume) of dendritic protrusions were observed exclusively in the basal, but not apical, dendrites of 17-month-old *Cyfp2* cKO mice. It is notable that changes in dendritic spine head width and size were also specifically observed in the basal, but not apical, dendrites of mPFC layer 5 neurons in adult (8–10-week-old) *Cyfp2* cKO mice (Zhang et al. 2020). Furthermore, our present study also revealed reduced length only in the basal, but not apical,

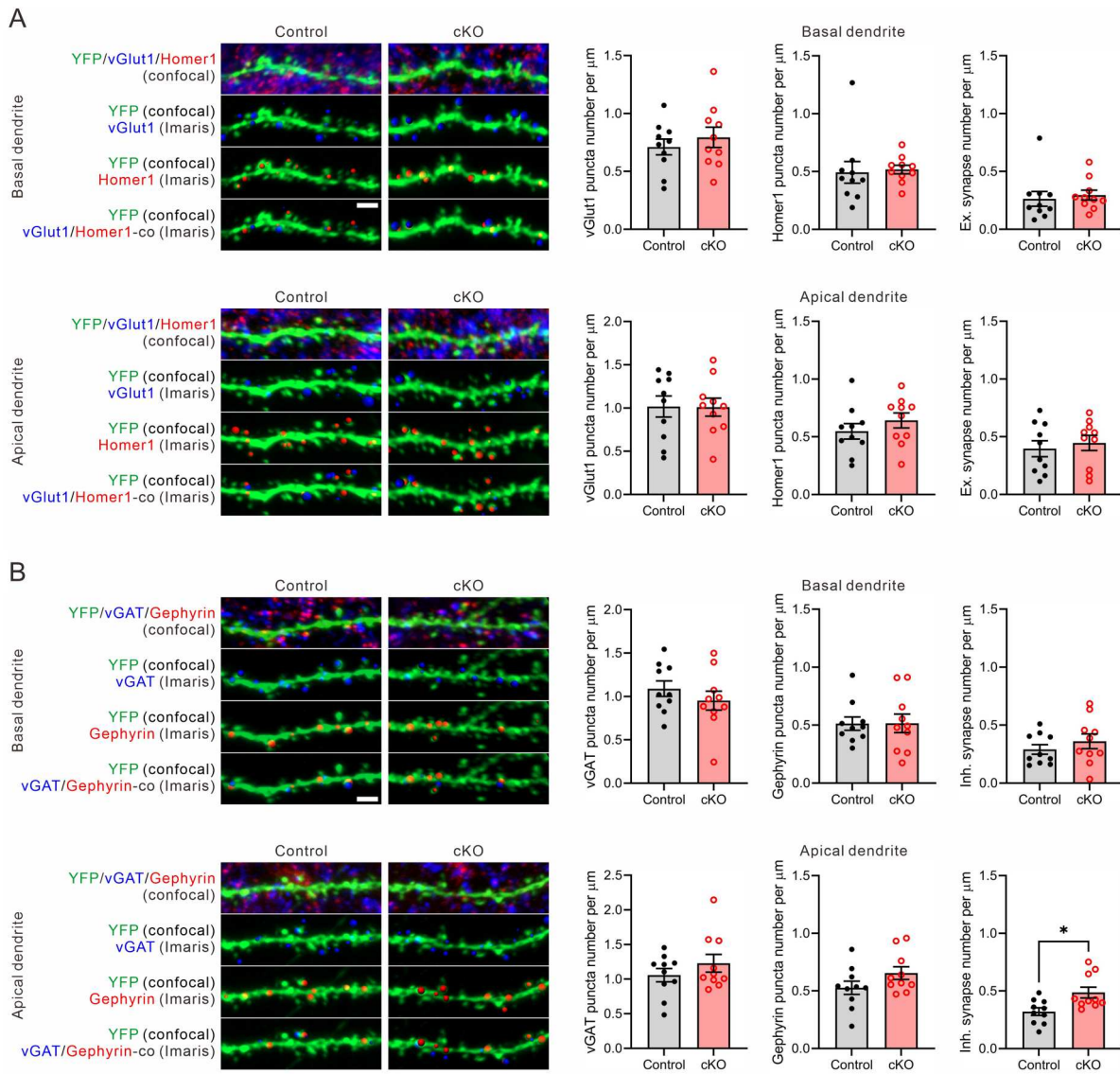


**Figure 3.** Excitatory and inhibitory synaptic densities in CA1 pyramidal neurons of 17-month-old *Cyfip2* cKO mice. (A) Representative confocal images of excitatory synapses and their Imaris detections in both basal (upper panels) and apical (lower panels) dendrites of CA1 pyramidal neurons of 17-month-old control and *Cyfip2* cKO mice. co, colocalization; Ex., excitatory. Scale bar, 2  $\mu$ m. Quantifications of densities of pre – (vGlut1) and post – (Homer1) synaptic markers and their colocalizations. (B) Representative confocal images of inhibitory synapses and their Imaris detections in both basal and apical dendrites of CA1 pyramidal neurons of 17-month-old control and *Cyfip2* cKO mice. Inh., inhibitory. Scale bar, 2  $\mu$ m. Quantifications of densities of pre – (vGAT) and post – (Gephyrin) synaptic markers and their colocalizations. N = 10 neurons per genotype.

dendrites of 17-month-old *Cyfip2* cKO mice. Intriguingly, in contrast, the number of inhibitory synapses (vGAT-Gephyrin colocalization) increased only in the apical, but not basal, dendrites of 17-month-old *Cyfip2* cKO mice. These findings suggest that the mechanisms underlying the regulation of neuronal morphology (i.e. dendrite length and dendritic protrusion morphology) and inhibitory synapse number by CYFIP2 could be distinct, with the former likely implicating the WRC-mediated regulation of actin polymerization and branching (Spence and Soderling 2015; Lee Y et al. 2017). However, the mechanisms for regulating inhibitory

synapses by CYFIP2 remain elusive. Previous studies demonstrated that exogenously expressed CYFIP2 localizes not only to excitatory but also to vGAT-Gephyrin-positive inhibitory synapses in cultured hippocampal neurons (Pathania et al. 2014; Davenport et al. 2019). Additionally, overexpression of CYFIP2 resulted in the downregulation of Gephyrin and GABA<sub>A</sub> receptor clusters in cultured hippocampal neurons (Davenport et al. 2019), suggesting that CYFIP2 localizes to and suppresses inhibitory synapses. This aligns with our observation of increased inhibitory synapse number in *Cyfip2* cKO mice. Moreover, we observed the localization

of endogenous CYFIP2 in dendritic spines (i.e. excitatory synapses) as well as the colocalization of CYFIP2 and Gephyrin in the hippocampal CA1 region of 17-month-old control mice (Supplementary Figure 2). One potential mechanism governing the localization and function of CYFIP2 in inhibitory synapses involves direct and/or indirect interactions of CYFIP2 with inhibitory synaptic proteins (Chen BY et al. 2014; Lee Y et al. 2020; Han KA and Ko 2023), though further investigations are needed to elucidate the details.

In conclusion, our findings contribute to the expanding list of neuronal phenotypes affected by cell-autonomous reduction of CYFIP2 in aged *Cyfp2* cKO mice, including changes in dendrite length, dendritic protrusion morphologies, and inhibitory synapse density. Investigating the interplay between CYFIP2 functions in CA1 pyramidal neurons and other hippocampal neurons, and their contribution to AD-like features in the hippocampus will be an intriguing avenue for future research. Such studies may offer the potential to uncover novel therapeutic targets.

## Disclosure statement

No potential conflict of interest was reported by the author(s).

## Funding

This work was supported by the National Research Foundation of Korea (NRF) grants funded by the Korea Government Ministry of Science and ICT (RS-2024-00399013 and RS-2024-00334487, NRF-2022R111A1A01053508) and by Korea University grants (K2401511 and K2405481).

## ORCID

Kihoon Han  <http://orcid.org/0000-0002-5925-2152>

## References

- Abekhouk S, Bardoni B. 2014. CYFIP family proteins between autism and intellectual disability: links with Fragile X syndrome. *Front Cell Neurosci.* 8. doi:10.3389/fncel.2014.00081.
- Begemann A, Sticht H, Begtrup A, Vitobello A, Faivre L, Banka S, Alhaddad B, Asadollahi R, Becker J, Bierhals T, et al. 2021. New insights into the clinical and molecular spectrum of the novel CYFIP2-related neurodevelopmental disorder and impairment of the WRC-mediated actin dynamics. *Genet Med.* 23(3):543–554. doi:10.1038/s41436-020-01011-x.
- Chen BY, Brinkmann K, Chen ZC, Pak CW, Liao YX, Shi SY, Henry L, Grishin NV, Bogdan S, Rosen MK. 2014. The WAVE regulatory complex links diverse receptors to the actin cytoskeleton. *Cell.* 156(1-2):195–207. doi:10.1016/j.cell.2013.11.048.
- Chen ZC, Borek D, Padrick SB, Gomez TS, Metlagel Z, Ismail AM, Umetani J, Billadeau DD, Otwinowski Z, Rosen MK. 2010. Structure and control of the actin regulatory WAVE complex. *Nature.* 468(7323):533–U207. doi:10.1038/nature09623.
- Choi SY, Han K, Cutforth T, Chung W, Park H, Lee D, Kim R, Kim MH, Choi Y, Shen K, et al. 2015. Mice lacking the synaptic adhesion molecule Neph2/Kirrel3 display moderate hyperactivity and defective novel object preference. *Front Cell Neurosci.* 9:283.
- Cioni JM, Wong HHW, Bressan D, Kodama L, Harris WA, Holt CE. 2018. Axon-axon interactions regulate topographic optic tract sorting via CYFIP2-dependent WAVE complex function. *Neuron.* 97(5):1078–107+. doi:10.1016/j.neuron.2018.01.027.
- Davenport EC, Szulc BR, Drew J, Taylor J, Morgan T, Higgs NF, Lopez-Domenech G, Kittler JT. 2019. Autism and schizophrenia-associated CYFIP1 regulates the balance of synaptic excitation and inhibition. *Cell Rep.* 26(8):2037–2051 e2036. doi:10.1016/j.celrep.2019.01.092.
- De Rubeis S, Pasciuto E, Li KW, Fernandez E, Di Marino D, Buzzi A, Ostroff LE, Klann E, Zwartkuis FJ, Komiyama NH, et al. 2013. CYFIP1 coordinates mRNA translation and cytoskeleton remodeling to ensure proper dendritic spine formation. *Neuron.* 79(6):1169–1182. doi:10.1016/j.neuron.2013.06.039.
- Ghosh A, Mizuno K, Tiwari SS, Proitsi P, Gomez Perez-Nievas B, Glennon E, Martinez-Nunez RT, Giese KP. 2020. Alzheimer's disease-related dysregulation of mRNA translation causes key pathological features with ageing. *Transl Psychiatry.* 10(1):192. doi:10.1038/s41398-020-00882-7.
- Han K, Chen H, Gennarino VA, Richman R, Lu HC, Zoghbi HY. 2015. Fragile X-like behaviors and abnormal cortical dendritic spines in cytoplasmic FMR1-interacting protein 2-mutant mice. *Hum Mol Genet.* 24(7):1813–1823. doi:10.1093/hmg/ddu595.
- Han KA, Ko J. 2023. Orchestration of synaptic functions by WAVE regulatory complex-mediated actin reorganization. *Exp Mol Med.* 55(6):1065–1075. doi:10.1038/s12276-023-01004-1.
- Kanellopoulos AK, Mariano V, Spinazzi M, Woo YJ, McLean C, Pech U, Li KW, Armstrong JD, Giangrande A, Callaerts P, et al. 2020. Aralar sequesters GABA into hyperactive mitochondria, causing social behavior deficits. *Cell.* 180(6):1178–+. doi:10.1016/j.cell.2020.02.044.
- Kang M, Zhang Y, Kang HR, Kim S, Ma R, Yi Y, Lee S, Kim Y, Li H, Jin C, et al. 2023. CYFIP2 p.Arg87Cys causes neurological defects and degradation of CYFIP2. *Ann Neurol.* 93(1):155–163. doi:10.1002/ana.26535.
- Kim GH, Zhang Y, Kang HR, Lee SH, Shin J, Lee CH, Kang H, Ma R, Jin C, Kim Y, et al. 2020. Altered presynaptic function and number of mitochondria in the medial prefrontal cortex of adult *Cyfp2* heterozygous mice. *Mol Brain.* 13(1):123. doi:10.1186/s13041-020-00668-4.
- Kim HJ, Kim J, Choi J, Sun W. 2022. Chemical fluorescence-based dye staining for 3-dimensional histopathology analysis. *Anim Cells Syst (Seoul).* 26(2):45–51. doi:10.1080/19768354.2022.2049641.
- Konietzny A, Bar J, Mikhaylova M. 2017. Dendritic actin cytoskeleton: structure, functions, and regulations. *Front Cell Neurosci.* 11:147. doi:10.3389/fncel.2017.00147.
- Kulkarni VA, Firestein BL. 2012. The dendritic tree and brain disorders. *Mol Cell Neurosci.* 50(1):10–20. doi:10.1016/j.mcn.2012.03.005.



- Lee B, Zhang Y, Kim Y, Kim S, Lee Y, Han K. 2017. Age-dependent decrease of GAD65/67 mRNAs but normal densities of GABAergic interneurons in the brain regions of Shank3-overexpressing manic mouse model. *Neurosci Lett*. 649:48–54. doi:10.1016/j.neulet.2017.04.016.
- Lee SH, Zhang Y, Park J, Kim B, Kim Y, Lee SH, Kim GH, Huh YH, Lee B, Kim Y, et al. 2020. Haploinsufficiency of *Cyfp2* causes lithium-responsive prefrontal dysfunction. *Ann Neurol*. 88(3):526–543. doi:10.1002/ana.25827.
- Lee Y, Kim D, Ryu JR, Zhang Y, Kim S, Kim Y, Lee B, Sun W, Han K. 2017. Phosphorylation of CYFIP2, a component of the WAVE-regulatory complex, regulates dendritic spine density and neurite outgrowth in cultured hippocampal neurons potentially by affecting the complex assembly. *Neuroreport*. 28(12):749–754. doi:10.1097/WNR.0000000000000838.
- Lee Y, Zhang Y, Kang H, Bang G, Kim Y, Kang HR, Ma R, Jin C, Kim JY, Han K. 2020. Epilepsy- and intellectual disability-associated CYFIP2 interacts with both actin regulators and RNA-binding proteins in the neonatal mouse forebrain. *Biochem Biophys Res Commun*. 529(1):1–6. doi:10.1016/j.bbrc.2020.05.221.
- Ma R, Pang K, Kang H, Zhang Y, Bang G, Park S, Hwang E, Ryu JR, Kwon Y, Kang HR, et al. 2022. Protein interactome and cell-type expression analyses reveal that cytoplasmic FMR1-interacting protein 1 (CYFIP1), but not CYFIP2, associates with astrocytic focal adhesion. *J Neurochem*. 162(2):190–206. doi:10.1111/jnc.15622.
- Ma R, Zhang Y, Li H, Kang HR, Kim Y, Han K. 2023. Cell-autonomous reduction of CYFIP2 is insufficient to induce Alzheimer's disease-like pathologies in the hippocampal CA1 pyramidal neurons of aged mice. *Anim Cells Syst (Seoul)*. 27(1):93–101.
- Mehder RH, Bennett BM, Andrew RD. 2020. Morphometric analysis of hippocampal and neocortical pyramidal neurons in a mouse model of late onset Alzheimer's disease. *J Alzheimers Dis*. 74(4):1069–1083. doi:10.3233/JAD-191067.
- Napoli I, Mercaldo V, Boyl PP, Eleuteri B, Zalfa F, De Rubeis S, Di Marino D, Mohr E, Massimi M, Falconi M, et al. 2008. The fragile X syndrome protein represses activity-dependent translation through CYFIP1, a new 4E-BP. *Cell*. 134(6):1042–1054. doi:10.1016/j.cell.2008.07.031.
- Oguro-Ando A, Rosensweig C, Herman E, Nishimura Y, Werling D, Bill BR, Berg JM, Gao F, Coppola G, Abrahams BS, et al. 2015. Increased CYFIP1 dosage alters cellular and dendritic morphology and dysregulates mTOR. *Mol Psychiatry*. 20(9):1069–1078. doi:10.1038/mp.2014.124.
- Pathania M, Davenport EC, Muir J, Sheehan DF, Lopez-Domenech G, Kittler JT. 2014. The autism and schizophrenia associated gene CYFIP1 is critical for the maintenance of dendritic complexity and the stabilization of mature spines. *Transl Psychiat*. 4:e374.
- Rottner K, Stradal TEB, Chen BY. 2021. WAVE regulatory complex. *Curr Biol*. 31(10):R512–R517. doi:10.1016/j.cub.2021.01.086.
- Schenck A, Bardoni B, Moro A, Bagni C, Mandel JL. 2001. A highly conserved protein family interacting with the fragile X mental retardation protein (FMRP) and displaying selective interactions with FMRP-related proteins FXR1P and FXR2P. *P Natl Acad Sci USA*. 98(15):8844–8849. doi:10.1073/pnas.151231598.
- Spence EF, Soderling SH. 2015. Actin out: regulation of the synaptic cytoskeleton. *J Biol Chem*. 290(48):28613–28622. doi:10.1074/jbc.R115.655118.
- Tiwari SS, Mizuno K, Ghosh A, Aziz W, Troakes C, Daoud J, Golash V, Noble W, Hortobagyi T, Giese KP. 2016. Alzheimer-related decrease in CYFIP2 links amyloid production to tau hyperphosphorylation and memory loss. *Brain*. 139(Pt 10):2751–2765. doi:10.1093/brain/aww205.
- Tsien JZ, Chen DF, Gerber D, Tom C, Mercer EH, Anderson DJ, Mayford M, Kandel ER, Tonegawa S. 1996. Subregion- and cell type-restricted gene knockout in mouse brain. *Cell*. 87(7):1317–1326. doi:10.1016/S0092-8674(00)81826-7.
- Zhang Y, Kang HR, Han K. 2019. Differential cell-type-expression of CYFIP1 and CYFIP2 in the adult mouse hippocampus. *Animal Cells Syst (Seoul)*. 23(6):380–383. doi:10.1080/19768354.2019.1696406.
- Zhang Y, Kang Hyae R, Lee SH, Kim Y, Ma R, Jin C, Lim JE, Kim S, Kang Y, Kang H, et al. 2020. Enhanced prefrontal neuronal activity and social dominance behavior in postnatal forebrain excitatory neuron-specific *Cyfp2* knock-out mice. *Front Mol Neurosci*. 13:574947. doi:10.3389/fnmol.2020.574947.
- Zhang Y, Lee Y, Han K. 2019. Neuronal function and dysfunction of CYFIP2: from actin dynamics to early infantile epileptic encephalopathy. *BMB Rep*. 52(5):304–311. doi:10.5483/BMBRep.2019.52.5.097.